Low-energy excitations of the correlation-gap insulator SmB_6: A light-scattering study

P. Nyhus and S. L. Cooper
Department of Physics and Frederick Seitz Materials Research Laboratory, University of Illinois, Urbana-Champaign, Urbana, Illinois 61801

Z. Fisk and J. Sarrao
Department of Physics and National High Magnetic Field Laboratory, Florida State University, Tallahassee, Florida 32306
(Received 6 November 1996)

We present the results of Raman scattering studies of single-crystal SmB_6 for temperatures down to 4 K and in magnetic fields up to 8 T. At temperatures below $T^* \sim 50$ K the electronic Raman continuum exhibits an abrupt redistribution of scattering intensity around a temperature-independent (''isobestic'') energy, $\Delta_c \sim 290\ \mathrm{cm}^{-1}$, reflecting the opening of a pseudogap which is larger than previously suggested by transport measurements. Additionally, the Raman response exhibits at least four well-defined excitations within the gap below T^*. The field dependencies of some of these in-gap states are consistent with the expected g factor ($g_{\mathrm{eff}}=2/7$) for the Sm^{3+} Γ_8 level, suggesting that these gap edge states are crystal-electric-field excitations of the Sm^{3+} ion split by magnetoelastic coupling. [S0163-1829(97)12717-5]

I. INTRODUCTION

A significant amount of condensed-matter research in the past two decades has been devoted to studying strongly correlated systems such as high-T_c cuprates, heavy-fermion compounds, Kondo insulators, and colossal magnetoresistance compounds, all of which are characterized by strong electron-electron and electron-phonon interactions which generate complex and varied ground and excited states. There has been particular interest recently in low carrier density Kondo systems such as $Ce_3Bi_4Pt_3$, YbB_{12}, CeNiSn, SmS, and SmB_6;[1] these materials behave like Kondo metals at high temperatures, but exhibit below a characteristic temperature T^* evidence for a small gap (or pseudogap) in the density of states, a nearly exponential suppression of the magnetic susceptibility, and in some cases strong electron-phonon coupling effects. That the gaps in these materials result from many-body, as opposed to band-structure, effects is supported in part by the observation that the energy scale, Δ, below which electronic states are renormalized by gap development in materials such as $Ce_3Bi_4Pt_3$ and SmB_6 is as much as 5–10 times larger than the characteristic temperature for gap development, T^*.[2,3]

SmB_6 is one of the most widely studied of these low carrier density Kondo systems. In the late 1960s, it was recognized that SmB_6 is homogeneous mixed-valent, with Mössbauer isomer shift,[4] lattice parameter, x-ray absorption,[5] and magnetic susceptibility measurements[6,7] showing that the Samarium ion at a single-crystallographic site fluctuates between two valence states, Sm^{2+} and Sm^{3+}, with a relative abundance of approximately 30 and 70%, respectively. The observation of a semiconductorlike resistivity[6,8,9] and a four-order-of-magnitude decrease in the carrier density between room temperature and 4 K (Ref. 9) first suggested the presence of a small gap in the density of states ($\Delta \sim 50$ K) at low temperatures in SmB_6. Direct spectroscopic probes, including infrared transmission[10,11] and reflectivity,[12] point contact spectroscopy,[13] and NMR measurements,[14,15] confirmed the presence of a gap in SmB_6 with an energy $\Delta \sim 30-150\ \mathrm{cm}^{-1}$. Similar gap energies have been inferred from specific-heat,[16] thermal expansion,[17] and elastic parameter measurements.[18] The magnetic susceptibility of SmB_6 is also interesting, exhibiting behavior typical of intermediate-valence compounds, including Curie-Weiss behavior for $T \gg T^*$, a broad maximum near T^*, and a rapid decrease in the susceptibility as $T \to 0$ (Refs. 6 and 7) (a low-temperature, $T < 10$ K, Curie tail often observed in measurements of SmB_6 is generally attributed to the presence of impurities).

A number of models have been proposed to account for the low-temperature properties of SmB_6. The mixed-valence nature of SmB_6 arises because the Sm $4f^6$ (Sm^{2+}) configuration lies close to the Fermi energy, allowing the $4f$ electrons to easily delocalize into the d band. Mott first suggested that the gap observed in systems such as SmB_6 forms when the dispersionless f-level hybridizes with the broad conduction band.[19] This so-called ''hybridization gap'' picture is typically described using the one-dimensional periodic Anderson model (PAM) Hamiltonian at half-filling. In the absence of a strong on-site Coulomb interaction, $U \to 0$, the PAM predicts a gap in the density of states due to coherent on-site hybridization between the f-level and the broad $5d$-$6s$ conduction band. One expects in this regime a small indirect gap associated with f-f-type transitions, as well as an optically-active direct f-d gap at higher energies. In the strong-coupling regime ($J \to \infty$), the PAM maps onto the Kondo lattice model, which in one-dimension has a ground state consisting of a lattice of local Kondo singlets comprised of conduction electrons bound to the localized magnetic moments. In this strong-coupling regime, excitations from the ground state include charge-gap excitations, Δ_c, associated with the unbinding of the conduction electron, and spin-gap excitations, Δ_s, between bound spin-singlet and -triplet configurations. Calculations of the one-dimensional (1D) asymmetric PAM indicate that the charge-gap energy can be sig-

nificantly larger than the spin-gap energy, $\Delta_c \sim 1.5\Delta_s - 2\Delta_s$, in this regime.[20,21]

Unfortunately, the 1D PAM model has limited success at describing the observed excitation spectrum of putative ''hybridization gap'' systems such as SmB_6. For example, Raman scattering measurements have shown that the characteristic temperature for gap development in SmB_6, $T^* \sim 50$ K[3] is substantially smaller than the energy scale (Δ) over which electronic states are affected, i.e., $\Delta \sim 8k_BT_c$, reflecting a ''phase-transition''-like character to gap development in SmB_6 which is not clearly described by the 1D PAM model. Similar behavior has also been observed in reflectance measurements of $Ce_3Bi_4Pt_3$.[2] Both neutron-scattering[22] and Raman-scattering[3] measurements of SmB_6 also reveal the presence of a 130-cm^{-1} in-gap resonance whose energy is roughly half of the gap energy observed in Raman scattering; that this excitation cannot be attributed to the simple singlet-to-triplet ($J=0 \rightarrow J=1$) ''spin-gap'' transition anticipated by 1D PAM calculations, however, is verified by the E, rather than T_1, symmetry observed for this excitation in these studies. An additional complication for 1D model predictions is that the neutron-scattering intensity of the 130-cm^{-1} in-gap resonance in SmB_6 exhibits a rapid Q dependence and a strong angular anisotropy, possibly indicating a substantial d-band character associated with this state. Indeed, Kikoin and Mishchenko have suggested that this excitation involves a transition between $4f^5 5d$ excitonic configurations.

Notably, several other interpretations of the ground and excited states in SmB_6 have been proposed, all stressing important features of low carrier Kondo systems which are not described by more conventional models such as the PAM. For example, Kasuya *et al.*[16] emphasize the importance of the small carrier density in SmB_6, arguing that the consequent enhancement of the Coulomb interaction energy relative to the kinetic energy makes conditions favorable for Wigner crystallization at low temperatures. Additionally, Kikoin and Mishchenko[23] (KM) have stressed the importance of d-f excitonic correlations in mixed-valence systems, proposing that SmB_6 and the high-pressure phase of SmS are unstable towards the formation of mixed-valence excitonic excited and ground states involving a $5d$ electron on nearest-neighbor Sm sites bound to a $4f$ hole on a central Sm atom. KM further suggest that these excitonic states have associated polaronic effects, since the large difference in the ionic radii of Sm^{2+} and Sm^{3+}, combined with the comparable energy scales of slow charge (valence) fluctuations and lattice vibrations, are conductive to strong electron-lattice coupling. Indeed, it is important to point out in this regard that SmB_6 exhibits numerous phonon anomalies compared to stable-valence isostructural rare-earth hexaborides. For example, neutron-scattering studies of SmB_6 reveal several lattice anomalies, including a softening of most phonon modes in SmB_6 compared to those of isostructural, integral valence LaB_6, anomalous dips in the dispersion of the LA phonons in the $[\xi\xi 0]$ and $[\xi\xi\xi]$ directions, and the existence of dispersionless ''gap'' modes between the acoustic and optical branches.[24] Raman scattering experiments[25,26] also show an ''extra'' phonon mode in SmB_6 which has been attributed to polaronic effects, and elastic measurements[18,27] find that the bulk modulus and the longitudinal elastic constant, c_{11}, in SmB_6 are anomalously soft compared with the reference material LaB_6. ''Soft'' and ''extra'' modes are also observed in other semiconducting intermediate valence compounds such as $Sm_{0.75}Y_{0.25}S$, ''gold'' SmS, and TmSe,[28–30] providing evidence that these lattice anomalies are a generic consequence of the complex electronic state of these materials. Notably, however, no evidence for polaronic effects has been observed in $Sm_{0.75}Y_{0.25}S$ by x-ray-diffraction techniques,[31] although similar measurements have, to our knowledge, not yet been performed in SmB_6.

In this paper, we report a detailed Raman-scattering investigation of the unconventional lattice and electronic properties of SmB_6. The complex interplay between electronic, spin, and lattice excitations in systems such as SmB_6 is naturally studied by Raman scattering, which not only offers an alternative to infrared spectroscopy as a direct means of probing energy gap development in this material, but also affords energy and symmetry information about other low-frequency excitations that may be important in ''hybridization gap'' systems, including crystal-field excitations, excitons, and anomalous phonons. As noted previously, our earlier Raman-scattering studies[3] showed not only that gap formation in SmB_6 involves a suppression of electronic scattering to energies as high as $\Delta \sim 290$ cm^{-1}, an energy which is much larger than the gap inferred from transport measurements, but also that gap development in SmB_6 occurs at temperatures much lower than the characteristic gap energy, $\Delta \sim 8k_BT^*$. In the more complete study presented here, we explore in greater detail the temperature-, symmetry-, and magnetic-field dependence of the gap in SmB_6. We also present a more complete investigation of the low-frequency in-gap resonance observed earlier in SmB_6, showing in particular that there is substantial ''fine structure'' associated with low-temperature in-gap states in SmB_6 which we believe reveals the substantial influence of local lattice distortions on the low-energy electronic states in this system.

II. EXPERIMENT

The cubic single crystals in this study were grown from an aluminum flux and measured typically 0.5–1.0 mm along the edges. The experiments described in this paper were performed using two different Raman systems. Most of the zero-field measurements were made with a SPEX 1877 subtractive triple spectrometer and an attached liquid-nitrogen-cooled Princeton Instruments CCD. Samples were excited with 20 mW of the linearly polarized 5145-Å line of an argon-ion laser incident on the sample at a pseudo-Brewster angle. The light was focused to a spot ~ 100 μm in diameter. A TRI liquid-helium bath cryostat cooled the samples down to 4 K. Spectra were obtained with the incident and scattered light polarized in the following configurations in order to identify the symmetries of the excitations studied: $(\mathbf{E}_i,\mathbf{E}_s)=(\mathbf{x},\mathbf{x}), A_{1g}+E_g$; $(\mathbf{E}_i,\mathbf{E}_s)=(\mathbf{x},\mathbf{y}), T_{1g}+T_{2g}$; $(\mathbf{E}_i,\mathbf{E}_s)=(\mathbf{x}+\mathbf{y},\mathbf{x}+\mathbf{y}), A_{1g}+1/4E_g+T_{2g}$; $(\mathbf{E}_i,\mathbf{E}_s)=(\mathbf{x}+\mathbf{y},\mathbf{x}-\mathbf{y}), 3/4E_g+T_{1g}$; where $\mathbf{E}_i$ and $\mathbf{E}_s$ are the incident and scattered electric-field polarizations, respectively, $\mathbf{x}$ and $\mathbf{y}$ are the [100] and [010] crystal directions, respectively, and $A_{1g}(\Gamma_1^+)$, $E_g(\Gamma_3^+)$, and $T_{2g}/T_{1g}(\Gamma_5^+/\Gamma_4^+)$, are the singly, doubly, and triply degenerate irreducible representations of the SmB_6 space group (O_h^1-$Pm3m$), respectively.

The magnetic-field experiments were carried out in a true backscattering geometry using a modified subtractive triple spectrometer with a Photometrics liquid-nitrogen-cooled CCD. The sample was cooled down to 1.5 K in a pumped Oxford flow cryostat which was mounted in the bore of an Oxford superconducting magnet. We used 10 mW of the linearly polarized 6471 Å krypton ion laser line for the zero-field measurements and circularly polarized light for the field-dependence measurements. The magnetic-field spectra were taken in the (RCP,LCP) and (RCP,RCP) geometries, where RCP and LCP refer to right and left circular polarization, respectively. The use of circularly polarized light was necessary for these magnetic-field measurements because the Faraday effect causes mixing of Raman symmetries for linearly polarized light. Circularly polarized laser light was obtained with a polarizing cube and a Berek compensator optimized for the frequency of the laser line. We analyzed the scattered light with a broadband quarter wave plate and a polarizing cube.

III. RESULTS AND DISCUSSION

A. Phonons and phonon anomalies

The room-temperature *unpolarized* Raman spectrum of SmB_6 shown in Fig. 1(a) exhibits four previously studied lattice modes and an electronic continuum which rises linearly up to a peak near 1000 cm^{-1}. We verified that the electronic continuum is indeed inelastic scattering, rather than luminescence, by exciting the samples with several laser excitation lines ranging from 6471 to 4765 Å and confirming that the continuum shifts appropriately for all excitation lines. The three first-order Raman-allowed modes in SmB_6 [see Fig. 1(a)] are observed at 730, 1100, and 1200 cm^{-1} and have symmetries T_{2g}, E_g, and A_{1g}, respectively. All these modes involve the displacement of boron atoms; the Sm ion is at a site of inversion symmetry and cannot contribute to first-order phonon Raman scattering.

A fourth peak with mainly E_g symmetry is also observed at 170 cm^{-1}. This ''extra'' mode is not allowed by the $Pm3m$ space group in first-order Raman scattering, and is particularly unusual in that it exhibits nearly an order of magnitude decrease in intensity between 300 and 40 K.[25] Similar modes have also been observed in the isostructural rare-earth hexaborides LaB_6, CeB_6, and NdB_6, (Ref. 32) but in SmB_6 the ''extra'' mode is significantly softer. Mörke *et al.* originally attributed the 170-cm^{-1} mode in SmB_6 to defect-allowed Raman scattering.[25] However, this interpretation does not account for the unusual temperature dependence of this excitation, for the fact that this mode is observed with undiminished strength even in the highest-quality samples, or for the absence of first-order defect-induced scattering in SmB_6, a feature typically observed in systems with strong defect scattering.[33] Rather, our temperature-dependence studies are consistent with recent measurements of SmB_6 (Ref. 26) which suggest that the low-frequency phonon Raman peak is largely due to two-phonon scattering. For example, Fig. 1(b) clearly shows that the intensity of the 170-cm^{-1} mode, $S(\omega)$, has a temperature dependence consistent with a two-particle thermal factor, i.e., $S(\omega)\sim[1+n(\omega/2)]^2$. Also, the position of the 170-cm^{-1} peak is very close to twice the energy of longitudinal acoustic phonons observed near the edge of the Brillouin zone by neutron scattering.

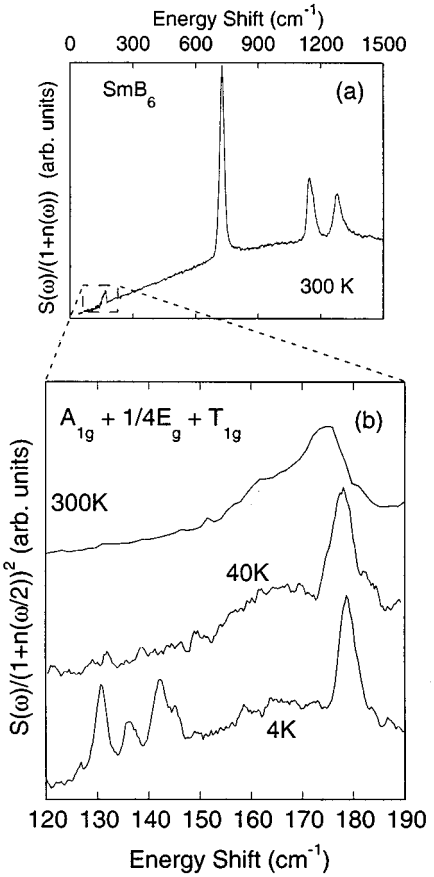

FIG. 1. (a) The unpolarized Raman response function of SmB_6 at 300 K, exhibiting (i) a linear continuum at low frequencies, (ii) T_{2g} (730 cm^{-1}), E_g (1148 cm^{-1}), and A_{1g} (1280 cm^{-1}) Raman-active optical phonons, (iii) and an ''extra'' mode at 174 cm^{-1}. (b) The 174 cm^{-1} mode intensity at 300, 40, and 4 K, illustrating a two-phonon temperature dependence. A two-phonon overtone thermal factor, $[1+n(\omega/2)]^2=[1-\exp(-\hbar\omega/2k_BT)]^{-2}$, has been divided from each spectrum and the spectra have been offset for comparison. The resulting integrated spectral weight of the 174 cm^{-1} mode changes little from 300 to 4 K, consistent with the interpretation of this mode as a two-phonon process. The peaks between $\sim$130 and $\sim$145 cm^{-1} in the 4 K spectrum are the low-temperature bound-state modes discussed in text.

The strong second-order phonon Raman scattering observed in SmB_6 is likely due to the same strong electron-phonon coupling effects that cause anomalies in the phonon dispersion curves of this compound. Klein has shown, in the context of narrow d-band systems such as TiN, TaC, and $NbSe_2$, that the two-phonon Raman matrix element is proportional under appropriate circumstances to the phonon self-energy associated with coupling to narrow-band electrons near the Fermi level, $\pi_q=\omega_q-\omega_{q0}$, where ω_q and ω_{q0} are the renormalized and unrenormalized phonon frequencies, respectively.[34] The two-phonon overtone Raman-scattering cross section, $R(2\omega_q)$, is, in such cases, directly proportional to the square of the phonon self-energy, $R(2\omega_q)\propto|\pi_q|^2$. In mixed-valence rare-earth systems such as SmB_6, strong phonon anomalies are expected due to the

strong coupling between lattice deformations and the fluctuating $4f$-$5d$ charge shells of the rare-earth (Sm) ion. Neutron-scattering studies of SmB_6 show that phonon anomalies in this system are strongest for longitudinal acoustic phonons in the [110] and [111] directions in the second half of the Brillouin zone where the dispersion is flat.[24] In the two-phonon Raman-scattering response, this should weight most heavily a narrow energy range of high-energy acoustic phonons in the second half of the Brillouin zone, accounting not only for the relative sharpness of the two-phonon scattering peak in SmB_6, but also for both the appearance of two-phonon scattering at roughly twice the energy of the most energetic acoustic phonons, and the absence of two-phonon scattering at lower frequencies.

Using a generalized charge-density distortion model, wherein an intermediate-valence excitonic state with soft valence fluctuations resonantly couples to different distortions of the lattice around the Sm^{3+} ion, Kikoin and Mishchenko (KM) have provided perhaps the most detailed interpretation of the origin of the unusual lattice properties of SmB_6.[35–37] KM find that the anomalies associated with the longitudinal acoustic phonons in the [110] and [111] directions in the second half of the Brillouin zone can be well described by monopolar (Γ_1^+) shell distortions associated with charge fluctuations between mixed-valence excitonic states, $\Psi_{g,e} = 4f^6 \pm 4f^5 5\tilde{d}$,[34] where $\tilde{d}$ represents an extended d state involving a superposition of d orbitals on nearest-neighbor Sm sites. Notably, the nonadiabatic coupling between phonons and charge fluctuations implicit in the KM model is also expected to give rise to hybrid excitations associated with both coherent and incoherent exciton-polarons.[36] For example, in the KM picture, incoherent polaronic distortions act like defects in the force constants of the crystal at temperatures above ~ 20 K, giving rise to local modes such as the 150-cm^{-1} dispersionless ''extra'' vibrational mode observed in neutron-scattering studies of SmB_6.[24]

The KM model also predicts that SmB_6 and similar mixed-valence systems should evidence ''local transitions'' between coherent exciton-polaron states involving propagating charge-density distortions resonantly coupled to ionic displacements. Recently, Lemmens *et al.* reported a T_{2g} contribution in the Raman spectra of SmB_6 near the 170-cm^{-1} ''extra'' mode which they attribute to such a local transition. It is not clear from our results if we see such a T_{2g} contribution in SmB_6. However, we have looked at the temperature dependence of the 170-cm^{-1} mode, finding that while the integrated spectral weight under this mode is well described by the two-phonon overtone thermal factor, $S(\omega) \sim [1-\exp(\hbar\omega/2kT)]^{-2} R''(\omega)$, there are at least two distinct components associated with this mode: a high-energy component near 180 cm^{-1} with a strongly temperature-dependent damping rate below 50 K, and a low-energy component near 165 cm^{-1} with a nearly temperature-independent linewidth [see Fig. 1(b)]. The sudden decrease in the damping rate of the 180 cm^{-1} component below $T^* \sim 60$ K does appear to betray a strong coupling of this excitation to low-energy charge degrees of freedom in SmB_6 (the relaxation of lattice modes due to traditional two-phonon decay should change little with temperature at low temperatures); unfortunately, our results do not reveal enough details about the nature of this coupling for a useful comparison to predictions of the KM model.

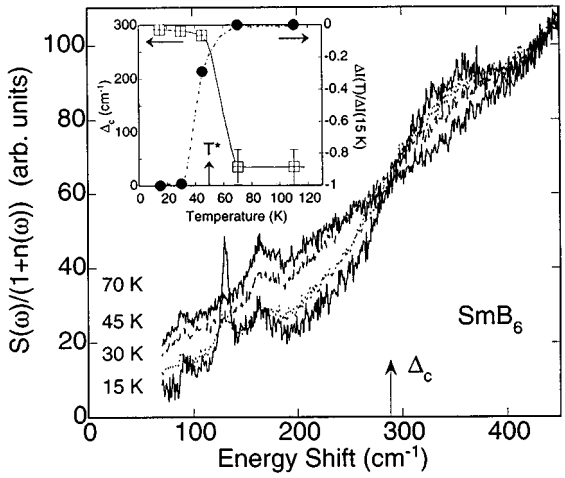

FIG. 2. Comparison of the low-frequency $A_{1g}+E_g$ symmetry Raman-scattering response function of SmB_6, $R''(\omega)=S(\omega)/[1+n(\omega)]$, from 70 to 15 K where $[1+n(\omega)]=[1-\exp(-\hbar\omega/kBT)]^{-1}$ is the thermal factor. The scattering response is suppressed below an isobestic point $\Delta_c \sim 290$ cm^{-1}, and redistributed above Δ_c between ~ 300 and 400 cm^{-1} as the gap develops. Also evident in the 15 and 30 K spectra is the $E_g(\Gamma_3^+)$ bound-state peak near 130 cm^{-1} which develops as the pseudogap forms. The inset shows comparison of the temperature dependence of the isobestic point (Δ_c) and the change in integrated spectral weight of gap, $\Delta I(T)/\Delta I(15\text{ K})$ (●). The spectral weight of each spectrum is integrated up to Δ_c and does not include the bound-state contributions. Δ_c (⊞) is the energy below which the spectrum loses intensity compared to the spectrum at the next highest temperature.

B. Gap development in SmB_6

1. Temperature dependence

The temperature dependence of the electronic Raman continuum in SmB_6 is shown in Fig. 2. The low-frequency ($\omega < 500$ cm^{-1}) continuum exhibits very little temperature dependence between 300 and 60 K. Below $T^* \sim 50$–60 K, however, electronic scattering intensity below 290 cm^{-1} is rapidly suppressed and redistributed to higher energies (with a peak energy of ~ 330 cm^{-1},) reflecting the development of a gap, or pseudogap, in the low-frequency excitation spectrum of SmB_6. The characteristic temperature, T^*, associated with gap development in Fig. 2 corresponds closely to the temperature at which the magnetic susceptibility has its maximum value,[6,8] and below which the resistivity increases with decreasing temperature.[6,8] Remarkably, the temperature dependence of the electronic Raman continuum in SmB_6 is characterized by a temperature-independent energy or ''isobestic'' point, $\Delta_c \sim 290$ cm^{-1}, across which electronic spectral weight is systematically transferred as the gap develops below T^*. Figure 2 also shows that the development of the gap in the electronic scattering response is accompanied by the appearance of a sharp E_g symmetry in-gap resonance which will be discussed in greater detail later.

While the development of a gap in SmB_6 has been observed in other measurements such as infrared reflectivity,

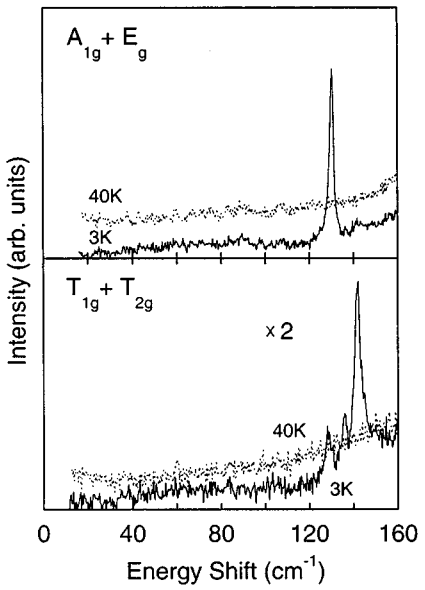

FIG. 3. In-gap resonances at 4 K, showing at least four peaks at 0 T, including $E_g(131\ \mathrm{cm}^{-1})$, $T_{2g}(142\ \mathrm{cm}^{-1})$, $T_{1g}(135\ \mathrm{cm}^{-1})$, and a weak fourth mode of T_{2g} or T_{1g} symmetry below $130\ \mathrm{cm}^{-1}$. The dashed lines compare the Raman response at 40 K.

transport, NMR, and point contact spectroscopy, our Raman-scattering results exhibit several interesting features which have not been revealed by other techniques. First, although transport and infrared transmission measurements of SmB_6 have infrared gaps of 30 and $140\ \mathrm{cm}^{-1}$, respectively, the Raman results shown in Fig. 2 demonstrate that gap development in SmB_6 influences electronic states up to a much larger energy, $\Delta_c \sim 290\ \mathrm{cm}^{-1}$, than is indicated by other measurements. Figure 3 shows in greater detail the influence of gap development on the low-frequency ($<130\ \mathrm{cm}^{-1}$) electronic scattering in SmB_6. Over the frequency range shown in Fig. 3 ($15-160\ \mathrm{cm}^{-1}$) gap development results in an abrupt, uniform suppression of electronic scattering; there is no feature in this spectrum at the reported energy of the transport gap, $\Delta_{\mathrm{tr}} \sim 30\ \mathrm{cm}^{-1}$, and only a slight ''kink'' in the slope of the Raman spectrum near the energy of the reported optical gap $\Delta_{\mathrm{opt}} \sim 130\ \mathrm{cm}^{-1}$. Thus, while the nearly complete suppression of electronic scattering due to gap formation is only observed for $\omega < 130\ \mathrm{cm}^{-1}$, Figs. 2 and 3 illustrate that gap development in SmB_6 influences electronic states up to much higher energies $\sim 290\ \mathrm{cm}^{-1}$. Notably, infrared measurements of SmB_6 not only reveal a low-temperature ($T < T^*$) transmission onset below $110\ \mathrm{cm}^{-1}$, but also clearly show that the opening of the gap in SmB_6 causes a partial suppression of the optical conductivity up to much higher energies, $\sim 240\ \mathrm{cm}^{-1}$, in reasonable agreement with our Raman results.

As we have reported previously,[3] a second significant feature of the low-temperature results in Figs. 1(b) and 2 is that the characteristic energy associated with gap development, defined by the isobestic point near $\Delta_c \sim 290\ \mathrm{cm}^{-1}$ (see Fig. 2), is nearly an order of magnitude larger than the characteristic temperature (T^*) below which the gap develops, i.e., $\Delta_c \sim 8 k_B T^*$. This behavior is more clearly illustrated in the inset of Fig. 2, which compares as a function of temperature the characteristic energy below which electronic scattering is suppressed, Δ_c, to the fractional change in the integrated electronic scattering strength below Δ_c, $\Delta I(T)/\Delta I(T = 15\ \mathrm{K})$, where $\Delta I(T) = I(T) - I(110\ \mathrm{K})$, and $I(T) = \int_0^{\Delta_f} R_e''(\omega, T) d\omega$ is the integrated spectral weight associated with the electronic contribution to the Raman-scattering response function $R_e''(\omega)$ below $\Delta_c \sim 290\ \mathrm{cm}^{-1}$ at a given temperature T. Figures 2 and 3 illustrate clearly that the low-energy electronic continuum changes little with temperature down to T^*, but decreases abruptly and over a wide frequency range below T^*.

The large difference between the characteristic energy, Δ_c, and the temperature scale at which the gap develops, T^*, in SmB_6 is also a property exhibited by other correlation gap systems, including FeSi and $Ce_3Bi_4Pt_3$. Significantly, this behavior is not consistent with that predicted by either ''fixed'' band-structure gap or simple ''hybridization'' gap descriptions. With respect to the latter, Sanchez-Castro *et al.*[38] have calculated the temperature dependence of the gap for the $U = \infty$ limit of the Anderson lattice Hamiltonian using a mean-field, slave-boson technique. In contrast to our observations in SmB_6, the hybridization gap energy in this calculation decreases gradually with increasing temperature and shows no evidence for a temperature-independent energy scale. A better comparison to our data is found in results of calculations by McQueen *et al.*,[39] which go beyond a mean-field treatment of the Anderson lattice Hamiltonian to include the effects of the temperature-dependent quasiparticle lifetime due to strong electron-electron scattering. These calculations predict that at high temperatures ($T \gg T^*$) the width of the quasiparticle spectral function is much larger than the renormalized hybridization gap, resulting in a smearing of the gap and ''dirty-metal'' transport behavior. As the temperature is reduced, however, the width of the quasiparticle spectral response decreases rapidly, and below a characteristic temperature T^* becomes less than the renormalized gap, resulting in pseudogap development. Calculations of the magnetic susceptibility using this model indicate a much stronger temperature dependence in the transition region than is expected in a conventional semiconductor, in agreement with our observations. Moreover, the results of these calculations are consistent with several key features of our Raman results, including the rapid development of a pseudogap below a temperature which is much less than the gap energy.

It is worth noting that various strong-coupling descriptions of mixed-valence insulators involving the formation of local bound states at low temperatures, including Kondo insulator (Kondo singlets) and excitonic insulator (excitons) pictures, appear at first glance to be consistent with certain aspects of our Raman results. In the strongly coupled Kondo insulator description, for example, the observation of a temperature-independent energy scale associated with gap development in SmB_6 could be identified with the Kondo temperature, T_K. Additionally, the 130-cm^{-1} in-gap resonance observed in SmB_6 is in certain respects reminiscent of a spin-flip transition (Δ_s) expected for a Kondo singlet state. For example, the spin-gap energy, $\Delta_s \sim 130\ \mathrm{cm}^{-1}$, and gap ratio, $\Delta_c/\Delta_s \sim 2.1$, implied by such an interpretation of our results are quite similar to those values inferred in the Kondo insulator $Ce_3Bi_4Pt_3$ from inelastic neutron-scattering and re-

TABLE I. Symmetries, energies, and field dependencies of in-gap excitations. The excitations denoted $a-f$ follow the labeling scheme in Fig. 6. Mode f appears weakly in the (RCP,RCP) polarization geometry.

Mode	Symmetry	ω (cm^{-1}) at 0 T	g_{eff} ($\Delta m_j=1$)
a	T_{2g} or T_{1g}	128.9	-0.15 ± 0.06
b	E_g	130.7	0.31 ± 0.04
c	T_{2g}	136.6 (at 2 T)	
d	Mostly T_{2g}	142.1	~ 0
e	E_g or T_{2g}		
f	T_{1g}	135.4	

flectivity experiments: $\Delta_s \sim 160\ \mathrm{cm}^{-1}$ and gap ratio $\Delta_c/\Delta_s \sim 1.8$, and is also consistent with 1D PAM calculations which find that $\Delta_c \sim \Delta_s$ to $2\Delta_s$.[21] However, as we shall discuss more completely in Sec. III C, the predictions of these 1D calculations cannot account for the complex ''fine structure'' and symmetries observed for the in-gap resonances in SmB_6, and thus these predictions are ultimately not consistent with our data. Rather, as we discuss below, our results suggest not only that the gap-edge states observed in SmB_6 have strong local moment character reminiscent of the Sm^{3+} $4f$ states, but also that these states are strongly influenced by magnetoelastic coupling effects which are not typically accounted for in electronic models of low carrier density Kondo systems such as SmB_6.

C. In-gap bound states

1. Temperature dependence

Perhaps the most remarkable consequence of pseudogap development in SmB_6 is the evolution of several resonances in the pseudogap (i.e., with energy less than Δ_c) below T^*. Figure 3 shows that there are, in fact, as many as four excitations which develop in the pseudogap below T^*: a strong, narrow E_g symmetry excitation at $130\ \mathrm{cm}^{-1}$, a strong, asymmetric T_{2g} symmetry excitation at $142\ \mathrm{cm}^{-1}$, and weaker T_{1g} and T_{2g} symmetry excitations at 136 and $128\ \mathrm{cm}^{-1}$, respectively. Table I summarizes this information. As shown in Fig. 3, all of these excitations share the same temperature dependence, namely a rapid diminution of intensity as temperature approaches T^*, suggesting that these excitations have a similar origin and are strongly damped by thermally excited d electrons in the conduction band. Interestingly, inelastic-neutron-scattering measurements[22] have also reported a single, broad (FWHM$\sim 16\ \mathrm{cm}^{-1}$) magnetic excitation in SmB_6 with the same temperature dependence and energy scale ($\sim 130\ \mathrm{cm}^{-1}$ at the Brillouin zone center) as the in-gap excitations we observe in Raman (open squares in Fig. 4). Our higher resolution Raman results consequently reveal that there is actually substantial ''fine structure'' associated with this excitation in SmB_6.

Several interpretations of the in-gap excitations we observe in SmB_6 are by themselves insufficient to account for either the number or symmetry of excitations observed, including (i) a simple $\Gamma_7 \rightarrow \Gamma_8$ crystal-field transition, (ii) an intermultiplet transition between spin-orbit split levels of either Sm^{3+} ($J=5/2\rightarrow 7/2$) or Sm^{2+} ($J=0\rightarrow 1$),[40] and (iii) a $J=0\rightarrow 1$ spin-flip transition, such as that predicted between different $4f^5 5d$ configurations by Kikoin and Mishchenko.[35] Rather, the rich spectrum of in-gap resonances observed in these measurements suggest strongly that magnetoelastic coupling, in addition to having an important influence on the lattice dynamics of SmB_6,[24,37,41] also has an important effect on the low-energy electronic states of this material. Several possibilities appear to be consistent with our results: (i) magnetoelastic splitting of spin-orbit split levels, similar to that reported previously in $Sm_{0.75}Y_{0.25}S$ (Ref. 42), (ii) magnetoelastic splitting of $4f^5 5d$ excitonic states,[35] or (iii) magnetoelastic coupling to crystal-electric-field (CEF) excitations.

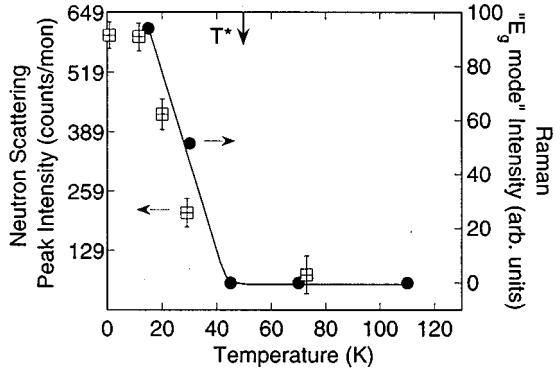

FIG. 4. Comparison of the temperature dependence of the $130\ \mathrm{cm}^{-1}$ magnetic excitation intensity measured by inelastic neutron scattering (⊞) (Ref. 50) and Raman scattering (●).

In order to further examine these possibilities, it is useful to first note that there are anomalous phonons which do appear to participate in strong magnetoelastic coupling in SmB_6. For example, the frequency of the T_{2g} Raman-active optical phonon in SmB_6 is substantially renormalized compared to the T_{2g} modes in stable-valence REB_6 compounds, suggesting a particularly strong coupling between T_{2g} symmetry lattice distortions and the low-frequency electronic states of SmB_6.[32] Moreover, although neutron-scattering results show a general softening of all modes in SmB_6 compared to other hexaborides, these measurements also find kinks in the dispersion of the longitudinal acoustic phonons near the Λ and Σ points of the Brillouin zone[24] which have significant local T_{2g} character. The anomalous behavior associated with the T_{2g} phonon in SmB_6 motivates two magnetoelastic coupling descriptions that are consistent with observed features of the in-gap bound states in SmB_6. First, a dynamical Jahn-Teller effect (DJTE), which causes a splitting of the Γ_8 crystal-field quartet by a T_{2g} symmetry phonon, and results in the formation of four hybrid states having symmetries $(\Gamma_8 \otimes T_{2g} =)\Gamma_6+\Gamma_7+2\Gamma_8$ and different mixtures of electron-phonon character. Notably, the presence of a DJTE has also been inferred from ESR measurements of Er^{3+}-doped SmB_6.[43,44] A second possibility is that magnetoelastic coupling causes a bound state between a T_{2g} phonon and both the Γ_7 and Γ_8 levels, similar to that proposed by Thalmeier *et al.*[45] to explain the observation of fine structure in the $\Gamma_7-\Gamma_8$ transition of $CeAl_2$ (Ref. 46). In the model of Thalmeier *et al.*, T_{2g} phonons near the X point of the Brillouin zone couple to the crystal-field levels, producing addi-

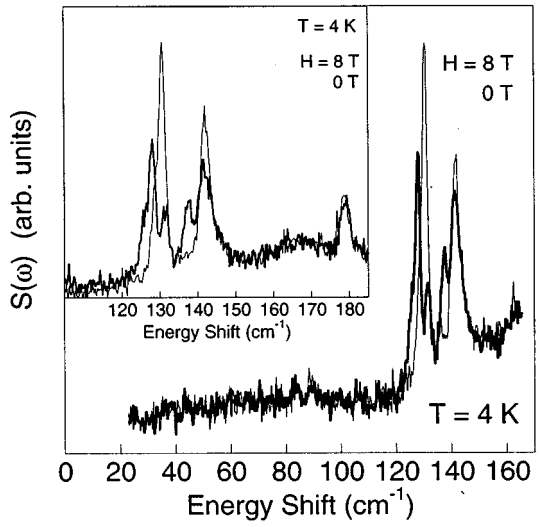

FIG. 5. The magnetic-field dependencies of the gap and defect modes. The thin line shows the gap and bound states at 4 K in zero field, while the thick line shows the low-frequency spectrum at 4 K in a 8-T field. The inset shows the same spectra in the range 120–185 cm^{-1}.

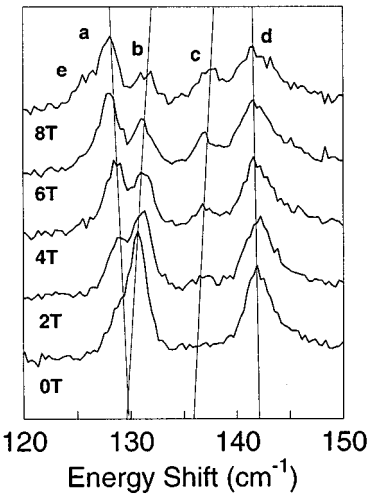

FIG. 6. The magnetic-field dependencies of the bound states. The plot shows (LCP,RCP) spectra for fields up to 8 T at 4 K, clearly showing the splitting of the E_g mode into at least two peaks denoted *a* and *b*. The straight lines through the peaks are guides for the eye. The 142-cm^{-1} T_{2g} mode (*d*) does not shift and appears to lose spectral weight with field to mode *c*. Mode *c* is not evident in the 0-T spectrum. Spectra have been offset for comparison. Peak fit parameters are summarized in Table I.

tional structure in the neutron-scattering spectrum. This description differs from the DJTE scenario in that the T_{2g} mode couples to both the Γ_7 and Γ_8 levels, resulting in the formation of three new hybrid states, including one of principally phononic character and two of primarily electronic character.

Notably, several properties of the in-gap states are consistent with the presence of magnetoelastic coupling. First, the reasonably strong Raman-scattering intensities associated with these in-gap states suggest the presence of some phonon character. Second, strong magnetoelastic coupling provides a natural explanation for the strong angle and $|\mathbf{Q}|$ dependence of the 130-cm^{-1} in-gap mode.[22] Finally, as discussed below, the magnetic field dependence of the in-gap resonances in SmB_6 affords additional evidence not only that these states are hybrid states with mixed electron-phonon character, but also that the electronic contributions to these states may be derived from the Sm^{3+} $4f^5$ crystal-field levels (Γ_7,Γ_8).[47]

2. Magnetic field dependence

The magnetic-field dependence of the low-frequency excitation spectrum in SmB_6 also affords insight into the nature of the in-gap states observed in this system. Most electronic models of the Kondo insulators predict a narrowing of the gap with field; for example, the simple hybridization gap picture predicts a narrowing of the gap which varies linearly with field due to Zeeman splitting of the localized gap-edge states. Experimentally, however, a large variation in the field dependence of different putative Kondo insulators has been observed. For example, YbB_{12} exhibits a large negative magnetoresistance and a rapid reduction of the gap with field which results in a field-induced insulator-to-metal transition at $H=45$ T. By contrast, SmB_6 exhibits a very small negative magnetoresistance, and has a gap that is reduced by only 4% in an 18-T field. Sugiyama *et al.*[48] have proposed that the different field dependencies observed in YbB_{12} and SmB_6 are wholly attributable to the different Landé g factors in Yb^{3+} ($g_{\rm eff}\sim 7/2$) (Ref. 47) and Sm^{3+} ($g_{\rm eff}=2/7$) ions, and are therefore consistent with an extended hybridization gap model. However, Cooley *et al.*[49] argue that the magnetoresistance in SmB_6 is too small to be accommodated by the hybridization gap description, and suggest instead that this behavior results from strong exchange coupling, which creates band edge states that are nonmagnetic singlets similar to those expected in a Mott-Hubbard insulator.

In order to provide a more detailed picture of the gap and in-gap states in SmB_6, we have studied the field dependencies of the pseudogap and resonance states observed using Raman scattering. Figure 5 shows that within the noise level of our data, we observe no field dependence in either the electronic continuum intensity within the pseudogap ($\omega < \Delta_c \sim 290$ cm^{-1}) or in the characteristic energy (''isobestic point''), Δ_c, for fields as high as 8 T. On the other hand, Fig. 6 illustrates significant changes in the spectrum of in-gap states. For example, the 130-cm^{-1} E_g mode is strongly influenced by field, exhibiting a roughly 3-cm^{-1} splitting for a field of $H=8$ T. Using the relationship $\Delta=\Delta_0+g_{\rm eff}\mu_B H$, where Δ is the energy splitting, H is the magnetic field, μ_B is the Bohr magneton, and assuming $\Delta m_j=1$, we estimate from this splitting a value of $g_{\rm eff}\sim 0.31\pm 0.04$ for the E_g symmetry in-gap state. This estimate is quite close to the Landé g factor for the Γ_8 level of Sm^{3+}, $g_{\rm eff}=2/7$ (~ 0.29), providing additional evidence that the states which develop at the gap edge in SmB_6 have strong local moment character, and indeed are closely related to the Sm^{3+} Γ_8 and Γ_7 crystal-field split levels. The insensitivity of the 143-cm^{-1} T_{2g} mode to an applied magnetic field, on the other hand, is consistent with a predominantly phononic character for this mode and with the hybrid nature of the in-gap states in SmB_6.

D. Conclusions

In summary, we have investigated the development of both a low-temperature many-body gap and a rich spectrum of in-gap states in SmB_6. We find that the low-temperature ground state and excited states in SmB_6 share some similarities with characteristic states expected in the simple ''hybridization gap'' model. In particular, we observe a spectrum of gap-edge states at low temperatures which have strong local-moment (f-electron) character. While we cannot rule out the possibility that these in-gap states are Kondo or excitonic bound states predicted by certain strong-coupling models of Kondo insulators, the number, symmetries, and field dependencies of these in-gap states suggest that they are most likely due to $4f^5$ Sm^{3+} crystal-field levels (Γ_8,Γ_7) whose degeneracies are split by strong magnetoelastic coupling to local lattice distortions. Indeed, the number and symmetry of these states can be described quite well by assuming that the Sm^{3+} Γ_8 crystal field level is split via a dynamical Jahn-Teller distortion associated with a T_{2g} phonon. Consequently, our results suggest that the in-gap states in SmB_6 are most appropriately viewed as ''phonon bound states'' caused by strong magnetoelastic coupling between the f levels and local lattice distortions. Thus, in addition to causing substantial anomalies in the elastic properties of SmB_6, strong electron-phonon coupling also has a significant influence on the low-energy electronic states of this compound.

On the other hand, the simple hybridization gap model completely fails to describe the dramatic, ''phase-transition''-like quality associated with charge gap development in SmB_6, this gap is characterized by a suppression of electronic scattering over an energy scale Δ_c that is substantially larger than the characteristic temperature T^* for gap development, $\Delta_c \sim 8k_BT^*$. Our measurements further indicate that gap development in SmB_6 renormalizes electronic states over a much wider energy than is suggested by the estimated transport gap. It is tempting to suggest that the dramatic development of the gap in SmB_6 is not primarily influenced by f-d hybridization, but rather by strong Coulomb correlations in the d band. The importance of such correlations is expected due to the low carrier densities in these materials, and indeed several groups have already noted the similarities between gap development in SmB_6 and that observed in Mott-Hubbard insulators.[49] It should also be pointed out, however, that calculations of the hybridization gap model which include quasiparticle electron-electron scattering effects also look promising for removing the discrepancies between our results and the predictions of simple hybridization gap models.

ACKNOWLEDGMENTS

This work was supported by the Department of Energy under Grant No. DEFG02-96ER4539 (P.N. and S.L.C.) and by the NHMFL through Grant No. NSF DMR 90-16241 (Z.F. and J.S.). We would like to acknowledge use of the MRL Laser Lab Facility, where much of this work was carried out, and we would also like to thank Miles Klein, Girsh Blumberg, and Moonsoo Kang for the use of their magnetic-field Raman system in portions of this work. Z.F. and J.S. acknowledge the partial support of the Japanese New Energy and Industrial Development Organization.

[1] G. Aeppli and Z. Fisk, Comments Condens. Matter Phys. **3**, 155 (1992).
[2] B. Bucher, Z. Schlesinger, P. C. Canfield, and Z. Fisk, Phys. Rev. Lett. **72**, 522 (1994).
[3] P. Nyhus, S. L. Cooper, Z. Fisk, and J. Sarrao, Phys. Rev. B **52**, 14 308 (1995).
[4] R. L. Cohen, M. Eibschütz, and K. W. West, Phys. Rev. Lett. **24** (1970).
[5] É. E. Vainshtein, S. M. Blokhin, and Y. B. Paderno, Sov. Phys. Solid State **6**, 2318 (1965).
[6] A. Menth and E. Buehler, Phys. Rev. Lett. **22**, 295 (1969).
[7] Y. B. Paderno, S. Pokrzywnicki, and B. Stalinski, Phys. Status Solidi **24**, K73 (1967).
[8] J. C. Nickerson, R. M. White, K. N. Lee, R. Bachmann, T. H. Geballe, and J. G. W. Hull, Phys. Rev. B **3**, 2030 (1971).
[9] J. W. Allen, B. Batlogg, and P. Wachter, Phys. Rev. B **20**, 4807 (1979).
[10] T. Nanba, H. Ohta, M. Motokawa, S. Kimura, S. Kunii, and T. Kasuya, Physica B **186-188**, 440 (1993).
[11] H. Ohta, R. Tanaka, M. Motokawa, S. Kunii, and T. Kasuya, J. Phys. Soc. Jpn. **60**, 1361 (1991).
[12] G. Travaglini and P. Wachter, Phys. Rev. B **29**, 893 (1984).
[13] I. Frankowski and P. Wachter, Solid State Commun. **41**, 577 (1982).
[14] O. Peña, M. Lysak, D. E. MacLaughlin, and Z. Fisk, Solid State Commun. **40**, 539 (1981).
[15] M. Takigawa, H. Yasuoka, Y. Kitaoka, T. Tanaka, H. Nozaki, and Y. Ishizawa, J. Phys. Soc. Jpn. **50**, 2525 (1981).
[16] T. Kasuya, K. Takegahara, T. Fujita, T. Tanaka, and E. Bannai, J. Phys. (Paris) Colloq. **40**, C-5 (1979).
[17] D. Mandrus, J. L. Sarrao, A. Lacerda, A. Migliori, J. D. Thompson, and Z. Fisk, Phys. Rev. B **49**, 16 809 (1994).
[18] A. Tamaki, T. Goto, S. Kunii, M. Kasaya, T. Suzuki, T. Fujimura, and T. Kasuya, J. Magn. Magn. Mater. **47&48**, 469 (1985).
[19] N. F. Mott, Philos. Mag. **30**, 403 (1974).
[20] K. Ueda, M. Sigrist, H. Tsunetsugu, and T. Nishino, Physica B **194-196**, 255 (1994).
[21] M. Guerrero and C. C. Yu, Phys. Rev. B **51**, 10 801 (1995).
[22] P. A. Alekseev, J.-M. Mignot, J. Rossat-Mignod, V. N. Lazukov, I. P. Sadikov, E. S. Konovalova, and Y. B. Paderno, J. Phys. Condens. Matter **7**, 289 (1995).
[23] K. A. Kikoin, J. Phys. C **17**, 6771 (1984).
[24] P. A. Alekseev *et al.*, Europhys. Lett. **10**, 457 (1989).
[25] I. Mörke, V. Dvorak, and P. Wachter, Solid State Commun. **40**, 331 (1981).
[26] P. Lemmens, A. Hoffmann, A. S. Mishchenko, M. Y. Talantov, and G. Güntherodt, Physica B **206&207**, 371 (1995).
[27] S. Nakamura, T. Goto, M. Kasaya, and S. Kunii, J. Phys. Soc. Jpn. **60**, 4311 (1991).
[28] H. A. Mook, R. M. Niklow, T. Penney, F. Holtzberg, and M. W. Shafer, Phys. Rev. B **18**, 2925 (1978).
[29] H. A. Mook, and F. Holtzberg, in *Valence Fluctuations in Solids*,

edited by L. M. Falicov, W. Hanke, and M. B. Maple (North-Holland, Amsterdam, 1981), p. 113.
[30] H. A. Mook, D. B. McWhan, and F. Holtzberg, Phys. Rev. B **25**, 4321 (1982).
[31] R. M. Martin, J. B. Boyce, and J. W. Allen, Phys. Rev. Lett. **44**, 1275 (1980).
[32] E. Zirngiebl, S. Blumenröder, R. Mock, and G. Güntherodt, J. Magn. Magn. Mater. **54-57**, 359 (1986).
[33] M. V. Klein, J. A. Holy, and W. S. Williams, Phys. Rev. B **17**, 1546 (1978).
[34] M. V. Klein, Phys. Rev. B **24**, 4208 (1981).
[35] K. A. Kikoin and A. S. Mishchenko, J. Phys. Condens. Matter **7**, 307 (1995).
[36] K. A. Kikoin and A. S. Mishchenko, JETP **77**, 828 (1993).
[37] K. A. Kikoin and A. S. Mishchenko, J. Phys. Condens. Matter **2**, 6491 (1990).
[38] C. Sanchez-Castro, K. S. Bedell, and B. R. Cooper, Phys. Rev. B **47**, 6879 (1993).
[39] P. G. McQueen and D. W. Hess, Phys. Rev. B **50**, 7304 (1994).
[40] P. A. Alekseev, V. N. Lazukov, R. Osborn, B. D. Rainford, I. P. Sadikov, E. S. Konovalova, and Y. B. Paderno, Europhys. Lett. **23**, 347 (1993).
[41] E. Zirngiebl and G. Güntherodt, in *Handbook on Physics and Chemistry of Rare Earths*, edited by K. A. Gschneidner and L. Eyring (North-Holland, Amsterdam, 1991), Vol. 14, p. 163.
[42] E. Holland-Moritz, E. Zirngiebl, and S. Blumenröder, Z. Phys. B **70**, 395 (1988).
[43] J. M. Dixon, J. Phys. C **10**, 833 (1977).
[44] H. Sturm, B. Elschner, and K.-H. Höck, Phys. Rev. Lett. **54**, 1291 (1985).
[45] P. Thalmeier and P. Fulde, Phys. Rev. Lett. **49**, 1588 (1982).
[46] M. Loewenhaupt, B. D. Rainford, and F. Steglich, Phys. Rev. Lett. **42**, 1709 (1979).
[47] A similar magnetoelastic splitting of the Γ_8 level was also inferred from the anomalous temperature dependence of a 370 cm^{-1} CEF Raman peak in CeB_6; see E. Zirngiebl, B. Hillebrands, S. Blumenröder, G. Güntherodt, M. Loewenhaupt, J. M. Carpenter, K. Winzer, and Z. Fisk, Phys. Rev. B **30**, 4052 (1984).
[48] K. Sugiyama, F. Iga, M. Kasaya, T. Kasuya, and M. Date, J. Phys. Soc. Jpn. **57**, 3946 (1988).
[49] J. C. Cooley, M. C. Aronson, A. Lacerda, Z. Fisk, P. C. Canfield, and R. P. Guertin, Phys. Rev. B **52**, 7322 (1995).
[50] P. A. Alekseev, J.-M. Mignot, J. Rossat-Mignod, V. N. Lazukov, and I. P. Sadikov, Physica B **186-188**, 384 (1993).